

## Twisted accretion discs – III. Application to Epsilon Aurigae

Sanjiv Kumar<sup>★</sup> *Institute of Astronomy, Madingley Road, Cambridge CB3 0HA*

Accepted 1986 October 23. Received 1986 October 23; in original form 1986 April 10

**Summary.** Twisting and alignment in a steady-state circumbinary accretion disc is studied. It is then used to account for observed features in the scenario of Epsilon Aurigae as a triple. The alignment depends on viscosity in the disc, but it is always substantial and leads to a tilted slab-like profile when viewed edge-on.

### 1 Introduction

The recent eclipse observations of Epsilon Aurigae have regenerated interest in explaining the unusual features of the eclipse light curves of this system. The difficulties in accounting for the observations have of late been alleviated by the proposal that this is a triple system comprising a short-period binary in orbit around an F0Ia supergiant (Eggleton & Pringle 1985). A central feature of this explanation is the presence of a twisted accretion disc, whose existence and behaviour is of interest to us. A similar suggestion has also been made based on the 27-yr-eclipse observations (Lissauer & Backman 1984).

In this paper, we show that thickening due to a twisted disc can account for the basic features of the light curves. This paper is a continuation of the earlier work on twisted accretion discs [Papaloizou & Pringle 1983 (PP); Kumar & Pringle 1985 (PI); Kumar 1985, 1986 (PII); refer to PI for the model]. The characteristic feature of the accretion disc in this system is that it is circumbinary. This affects the twisting features of the disc, which is of interest in its own right. The disc tilt is denoted by the complex quantity,  $W = W(R)$ , where  $R$  is the radius in cylindrical coordinates. Its magnitude and phase give the local inclination angle and the phase of the twisted disc. The disc is in steady state.

Application of the twisted disc model is limited by the formal requirement that the tilt angle is less than the disc opening angle. However we do not expect the qualitative features of the twisted disc to be affected substantially when this requirement is violated. A Lagrangian perturbation treatment is needed for accurate quantitative results, but in its absence the present model takes the viscous effects appropriately into account (see PP for a detailed discussion).

The introduction summarizes the current scenario and some alternative explanations. In Section 2 the magnitude of the precession frequency is estimated for a triple system. In Section 3, the problem of a twisted circumbinary disc is set up and applied to  $\epsilon$  Aur. The numerical results

<sup>★</sup> Present address: ICTP, SISSA, Bella Vista, 34100 Trieste, Italy.

are discussed in Section 4, and are used to obtain the twisted disc profile in Section 5. The conclusion is summarized in Section 6.

The observations show an eclipse depth of  $\sim 50$  per cent and there is a long, approximately constant minimum in the light curve. There is a gradual bump in the middle. Also the change in luminosity is not accompanied by the change in colour. To explain these eclipse depth and shape features, a cool and opaque disc was postulated as a companion to the supergiant (Huang 1965). The thickness of this disc is  $\sim$  the radius of the F supergiant  $R_F$ , which is  $\sim 150 R_\odot$ . The other dimension of the disc, its diameter  $\sim 8 R_F$ . The distance of  $\varepsilon$  Aur has been fixed at  $580 \pm 30$  pc (van der Kamp 1978). The mass function is  $\approx 3.1$  (Morris 1962). Wilson (1971) suggested an eclipsing thin disc with a large central hole to avoid the problem of luminosity required for the supergiant in Huang's model, and explain the bump in the light curve.

The possibility of  $\varepsilon$  Aur as a triple system is based on the suggestion of an evolutionary connection between a known triple HD 157978/9 (McLaughlin 1962) and this system (Eggleton & Pringle 1985). The HD system has a close binary of A stars (called \*11, \*12), which has an orbital period of  $\approx 3.76$  day. These two stars are of nearly equal masses orbiting round a red giant star (called \*2). This larger binary has an orbital period of 1170 day and an eccentricity  $e = 0.45$ ; the system is expected to circularize as the giant expands and approaches the Roche lobe.

It is assumed that for  $\varepsilon$  Aur (see Eggleton & Pringle 1985 for a summary of the observations and the triple model) the inclination of the close binary  $i_1 = 70^\circ$  so that the tilt of the disc is  $\approx 20^\circ$ . Precession leads to twisting and thence to a thick disc profile. They suggest an evolution scenario in which the supergiant mass  $\approx 1.3 M_\odot$  resides primarily in the degenerate carbon core, and the mass of the unseen companion  $\approx 5 M_\odot$ . Mass transfer to a single companion implies a rather short accretion time-scale. However if the mass transfer is to a close binary, then the matter has a larger accretion time-scale. This is because this close binary transfers angular momentum to the inner edge of the disc (Lin & Papaloizou 1979). Hence the accretion disc can cool to an opaque cloud.

An alternative evolution scenario, when the companion is not a binary, is also suggested by Eggleton & Pringle (1985). But binarity makes the long lifetime of the accretion disc after the mass transfer has stopped plausible. It avoids the need of a strong stellar wind preceding the Roche lobe overflow which the alternative scenario requires. Also the large luminosity of the earlier models (Huang 1965; Wilson 1971) is removed by having lower masses for the stars and a smaller, less luminous F0Ia supergiant. This is the scenario in which the possibility of a twisted disc giving rise to the obscuring object is considered. Since the mass transfer has been completed,  $\dot{M} = 0$ . Because the close binary prevents accretion the accretion disc is in a steady state.

The parallel suggestion (Lissauer & Backmann 1984) is that the F supergiant mass  $\sim 16 M_\odot$ , while the close binary stars have mass  $\sim 8 M_\odot$  each. The eclipse light curves suggest that the elongated secondary is 10 AU by  $\geq 1$  AU. They then find the larger binary orbital separation of  $\sim 30$  AU and the diameter of the primary  $\sim 2.6$  AU. Their suggestion for the observed primary as an F supergiant is based on its high luminosity, its radius determined from the eclipse timing and its effective temperature,  $T_{\text{eff}} \sim 7500\text{--}7800$  K. This gives a lower limit of  $12 M_\odot$  for the F star. They also suggest that the obscuring disc has a sharp outer edge, since the  $0.4\text{--}4 \mu\text{m}$  light curves have the same slope early in the ingress.

Two types of models have been recently suggested to account for the eclipse light curves. One approach is to understand the thin disc structure by tracking the path of an individual particle (van Hamme & Wilson 1986). The idea is to treat a restricted four-body problem, and study the orbit of a massless point particle as it precesses in the potential of a triple system. It is argued that out-of-phase radial incursions of a collection of particles could be the requisite viscosity mechanism. The measured temperature of the object  $\sim 500$  K (Backman *et al.* 1984), and the graininess are used to argue for an extremely thin disc. They rule out a twisted disc, and suggest a planar disc with an inclination of  $\sim 1^\circ$ . Here the disc is aligned with the inner binary. It is not clear

if the role of the viscosity is properly accounted for in this calculation. A many particle treatment of the settling of particles from out of plane to the symmetry plane of the inner binary is really required to address this problem fully.

The other is an analysis which attempts to match the *UBV* light curves and polarization observations with a geometrical disc model (Kemp *et al.* 1986). A slab geometry for the eclipsing disc with an aspect ratio of 11:1 (10:0.9 AU) is used to fit the data. The disc tilt is  $\sim 2^\circ$ . There is qualitative agreement, but quantitatively the dip in the light curve is less than observed, and with a smaller downslope.

## 2 Precession of the accretion disc

In this section we derive the form for precession which is applicable to the case of a circumbinary disc. This will be used in the following section to examine the behaviour of this disc when the close binary pair is inclined with respect to the larger orbital plane. We shall see that the quadrupole moment of the close binary is the most important contributor to the precession near the inner parts of the disc; while forced precession of the close binary and the recession of the nodes due to the quadrupole moment of the mass-losing star is important in the outer parts. This contrasts with the case of accretion on to a compact object where the quadrupole moment is always less than the Lense–Thirring effect by a factor of  $(R/R_*)^{1/2}$  and therefore neglected.

The close binary orbital period is assumed to be small, so that this binary can be treated as a plane circular ring. If the period is not assumed to be small, then we have to consider the potential due to three point masses, two of which are close. However in this case the azimuthal averaging of the potential gives the same result as before. Just as before, the effects of the larger orbital period are neglected.

Construct a coordinate system with its origin at the centre of mass of the close binary. The orbit is assumed to be circular and the stars have equal masses  $M_{11}=M_{12}=M$ , while the giant mass is  $M_2 \gg M$ . Take a ring with mass distribution  $2M \delta(r-a) \delta(\theta-\pi/2)$  where  $a$  is the ring radius; the ring lies in the equatorial plane. Then the potential at a field point  $P$ ,

$$V(\mathbf{r}) = -G \int dM/u, \quad (2.1)$$

where

$$u = |\mathbf{r} - \mathbf{r}_{\text{RING}}|.$$

Writing  $dM = \mu dl$ , so that  $\mu$  is the linear density of ring;  $\gamma = (\mathbf{r}, \mathbf{r}_{\text{RING}})$ , then

$$\begin{aligned} V(\mathbf{r}) &= -G \int \mu dl / \sqrt{r^2 + a^2 - 2ar \cos \gamma} \\ &= -\frac{4GM}{\pi r} \int_0^{\pi/2} d\phi_R \sum_{l=0}^{\infty} (a/r)^l P_l(\cos \gamma) \end{aligned} \quad (2.2)$$

where  $dl = a d\phi_R$ .

Now  $\cos \gamma = \cos \theta \cos \theta_R + \sin \theta \sin \theta_R \cos(\phi - \phi_R)$ . For  $\theta_R = \pi/2$ ,  $\cos \gamma = \sin \theta \cos \phi'$  ( $\phi' = \phi - \phi_R$ ).

Then

$$V(\mathbf{r}) = -\frac{2M}{r} \left[ 1 + \frac{a^2}{2r^2} (\frac{3}{2} \sin^2 \theta - 1) \right]. \quad (2.3)$$

If we consider three point masses, then

$$V(\mathbf{r}) = -G \sum_{i=1}^3 M_i \sum_{l=0}^{\infty} \frac{r_{<}^l}{r_{>}^{l+1}} P_l(\cos \gamma_i).$$

On expansion we find that (1) for

$$a_{11}, a_{12} \ll r \ll a_2, V(\mathbf{r}) = -\frac{2GM}{r};$$

(2) for

$$r \sim a_{11}, a_{12} \ll a_2, V(\mathbf{r}) = -\frac{2GM}{r} \left[ 1 + \frac{a^2}{r^2} (3 \sin^2 \theta \cos^2 \phi' - 1) \right];$$

and for (3)

$$a_{11}, a_{12} \ll r \ll a_2, V(\mathbf{r}) = -\frac{2GM}{r} - \frac{GM_2}{a_2} \left[ 1 + \frac{r}{a_2} (\cos \theta \sin i + \sin \theta \cos \phi) + \left( \frac{r}{a_2} \right)^2 (3 \sin^2 \theta \cos^2 \phi - 1) \right].$$

The precession contribution from the recession of nodes can be seen from case (3) after azimuthal averaging ( $M_2$  = mass of companion;  $r_{<}, r_{>}$  are the smaller, larger of the distances):

$$\omega_{\text{RN}} = \frac{1}{\Omega_{\text{K}} r^2 \cos \theta} \frac{\partial}{\partial \theta} \langle V(\mathbf{r}) \rangle_{\phi} = -\frac{3}{4a_2^2} \frac{GM_2}{(2GM)^{1/2}} r^{3/2} \quad (2.4)$$

where  $\Omega_{\text{K}}$  is the Keplerian angular velocity for the matter orbiting the close binary. The precession period then is

$$P_{\text{RN}} \sim \frac{4}{3} \frac{P_1^2}{P_2} \frac{M_{\text{T}}}{M_2} \left( \frac{a}{r} \right)^{3/2}$$

where  $P_1$  is the orbital period,  $P_2$  is the close binary orbital period and  $M_{\text{T}}$  is the triple mass.

For the inner regions of the disc, case (2) shows that

$$\omega_{\text{QM}} = \frac{1}{\Omega_{\text{K}} r^2 \cos \theta} \frac{\partial}{\partial \theta} \langle V(\mathbf{r}) \rangle_{\phi} = -\frac{3}{4} \Omega_{\text{K}} \left( \frac{a}{r} \right)^2. \quad (2.5)$$

This may be compared with the prograde precession frequency that arises due to the Lense–Thirring torquing of matter by the binary with separation  $2a$  and mass  $2M$  treated as a massive ring (Hatchett, Begelman & Sarazin 1981),

$$\omega_{\text{LTR}} \approx \left( \frac{4a^2 GM}{c^2 r^3} \right) \Omega_{\text{K}} \left[ 1 + 0.56 \left( \frac{G}{r} \right)^2 + 0.22 \left( \frac{G}{r} \right)^4 \right].$$

We see that for matter in the inner regions of the disc,

$$\frac{\omega_{\text{LTR}}}{\omega_{\text{QM}}} \sim \frac{R_g}{a} \ll 1$$

where

$$R_g = \frac{GM}{c^2}.$$

We estimate the dimensionless form of the precession parameters for Epsilon Aurigae. Using  $T = h^2 \Omega_* t$  as the viscous time coordinate, where  $h \equiv H_*/R_*$  and  $\Omega_* = \Omega_K$  (inner boundary),

$$\sigma_0 = \left( \frac{\omega}{h^2 \Omega_{K_i}} \right).$$

Then

$$\sigma_{\text{ORN}} \approx - \frac{3}{4h^2} \left( \frac{a}{a_2} \right)^3 \frac{M_2}{2M} T^{3/2} \quad (2.6)$$

where

$$r = \frac{R}{a}$$

is the dimensionless radial distance. Similarly

$$\sigma_{\text{OQM}} \sim - \frac{3}{4h^2} r^{-7/2}.$$

Using

$$a \sim 5 \times 10^{12} \text{ cm}, \quad a_2 \leq 10^{15} \text{ cm}, \quad M \sim 2M_\odot, \quad M_2 \sim 4M_\odot,$$

then

$$\sigma_{\text{ORN}} \approx - \frac{3}{4h^2} \frac{10^{-6}}{8} r^{3/2}.$$

Then  $\omega_{\text{ORN}} \approx 8\sigma_{\text{ORN}} = -10^{-4} r^{3/2}$  for  $h \approx 10^{-1}$ . Similarly  $\omega_{\text{OQM}} \sim 6 \times 10^2 r^{-7/2}$ .

We also need to consider the forced precession of the close binary. Since this effect is retrograde, the matter being added to the outer parts of the disc has a relative prograde precession. The quadrupole moment of the misaligned close binary leads to a precession of the larger orbital plane and the close binary is precessed in turn due to angular momentum conservation. As shown before,

$$\omega_{\text{orb}} \approx - \frac{3}{2} \left( \frac{a}{a_2} \right)^2 \Omega_{\text{orb}}.$$

From

$$\omega_{\text{orb}} M_2 a_2^2 \sim \omega_{\text{FP}} (2M) a^2,$$

we find that  $\omega_{\text{FP}} \sim \Omega_{\text{orb}}$ . Then

$$\sigma_{\text{OFP}} \sim \frac{\Omega_{\text{orb}}}{h^2 \Omega_*}$$

and

$$\omega_{\text{OFP}} \sim \frac{8}{h^2} \left( \frac{a}{a_2} \right)^{3/2}.$$

For the above parameters,  $\omega_{\text{OFP}} \sim 2 \times 10^{-1}$ . This calculation only gives an order of magnitude

since the precession frequency of the larger binary orbital period  $\sim$  orbital period, and the assumption used in deriving precession by neglecting the orbital effects are no longer valid.

Even though for steady-state disc configurations,  $\dot{M}$  is 0, the effects of forced precession cannot be neglected in our modelling of Epsilon Aurigae. The estimates calculated above are used in the twist equation in the following section.

### 3 The twisted disc in Epsilon Aurigae

We now apply the twisted disc theory to the possible triple system  $\epsilon$  Aur. The close binary system in this triple, which is comprised of the A stars, is inclined  $\approx 20^\circ$  to the larger orbital plane. This latter plane of the triple is seen edge-on so that its inclination is  $\approx 90^\circ$ . The accretion disc resulting from the Roche lobe overflow of the F0Ia supergiant is aligned with this mass-losing star at the outer radius, and presumably with the close binary at the inner radius. In this process, the disc gets warped, which can lead to the thickening required to eclipse the inner binary disc completely, as well as eclipse the supergiant every  $\sim 27$  years.

From the triple system model suggested (Eggleton & Pringle 1985), we get some of the required parameters. These are (i) the masses of the two A stars in the close binary  $M_{11} \sim M_{12} \sim 2M_\odot$ ; (ii) the mass of the supergiant  $M_2 \sim 4M_\odot$  (the difference here from the Eggleton & Pringle estimate by a factor of a few is not important. It turns out that  $\alpha$ -viscosity is the significant parameter; and (iii) the separation of the close binary and the supergiant  $a \sim 10^9 P^{2/3}$  where  $P \sim 9890$  day, which implies that the separation  $a \leq 10^{15}$  cm. The orbital period of the close binary is expected to be  $\sim$  a few days analogous to that of the close binary in the known triple system HD 157978/9, which has  $P_1 \leq 4$  day, and a separation of  $a_1 \leq 4 \times 10^{12}$  cm. The outer circumbinary radius of the warped accretion disc,  $R_0 \sim 10^2 R_*$ , the disc inner radius (compared to  $R_0 \sim 2R_*$  in the earlier model of Huang 1965; Wilson 1971), so that now using this outer disc radius  $\leq 10^{15}$  cm and the above listed parameters, we can estimate the magnitudes of the various relevant precession mechanisms, which in this context turn out to be forced precession and the recession of nodes. The former of these two is in fact more important.

Since the disc cannot accrete on to the close binary (which instead transfers angular momentum and energy to the disc), the steady-state equations for the surface density distribution of this accretion disc are different from those used earlier in the context of black holes and neutron stars. The equation for the radial distribution of the surface density,  $\Sigma$ , has been written down (see PI) as

$$\frac{3}{R} \frac{d}{dR} \left[ R^{1/2} \frac{d}{dR} (\nu \Sigma R^{1/2}) \right] + \frac{\dot{M}}{2\pi R_K} \delta(R - R_K) = 0. \quad (3.1)$$

In this equation, the second term describes the addition of mass at a constant rate,  $\dot{M}$  at a prescribed radius,  $R_K$ . The difference from the earlier types of accretion discs arises from the difference in the inner boundary condition imposed. Here both the inner and the outer boundary conditions reflect the vanishing of the radial drift velocity at these boundaries:

$$\frac{d}{dR} (\nu \Sigma R^{1/2}) = 0$$

since

$$V_R = - \frac{3}{\Sigma R^{1/2}} \frac{d}{dR} (\nu \Sigma R^{1/2}) = 0. \quad (3.2)$$

Transforming the radial variable  $R$  to  $z = R^{1/2}$ , and writing  $\gamma = \nu \Sigma R^{1/2}$  for the viscous term,

as before, we obtain the solution of the above equation for  $\Sigma$ :

$$\gamma = \begin{cases} c_1 + c_2 Z & Z_{\text{in}} \leq Z < Z_{\text{K}} \\ d_1 + d_2(z - z_0) & Z_{\text{K}} < Z \leq Z_{\text{OUT}} \end{cases} \quad (3.3)$$

where  $c_1$ ,  $c_2$ ,  $d_1$ ,  $d_2$  are arbitrary constants of integration and  $Z_{\text{K}} = R_{\text{K}}^{1/2}$ . From the boundary conditions

$$\frac{d\gamma}{dZ} = 0 \quad (3.4)$$

the matching condition at

$$Z_{\text{K}}, \gamma_{Z_{\text{K}}} = \gamma_{Z_{\text{K}}} \quad (3.5)$$

we find that

$$c_2 = d_2 = 0; \quad c_1 = d_1 \quad (3.6)$$

so that  $\gamma = \text{constant}$  is the required steady-state solution for the surface density distribution of this circumbinary disc, i.e.  $\dot{M}$  has to be 0 for a steady-state solution since no mass is flowing out of the inner edge of the disc.

We use this result to find  $\sigma$  for a disc with a constant opening angle  $h$ , where the viscosity follows the usual prescription:

$$\nu = \alpha h^2 R^2 \Omega.$$

Using the dimensionless radial variable

$$y \equiv \left( \frac{R}{R_*} \right)^{1/2}$$

the steady-state tilt equation becomes (Kumar 1985)

$$\frac{3\alpha}{4y^2} \left[ 1 - \frac{y^2}{\sigma} \frac{d}{dy} \left( \frac{\sigma}{y} \right) \right] - i\omega_p W = \frac{f^*(\alpha)}{8\sigma y} \frac{d}{dy} \left( \sigma \frac{dW}{dy} \right) \quad (3.7)$$

where

$$\sigma = \left( \frac{\Sigma}{\Sigma_*} \right) \left( \frac{R}{R_*} \right)^{3/2}.$$

Write

$$\nu \Sigma R^{1/2} = c;$$

then

$$\Sigma = \frac{c}{\alpha h^2 (GM)^{1/2} R}$$

and

$$\Sigma_* = \frac{c}{\alpha h^2 (GM)^{1/2} R_*},$$

so

$$\frac{\Sigma}{\Sigma_*} = \frac{1}{y^2} \quad \text{or} \quad \sigma = y.$$

Then the tilt advection velocity

$$V_{\text{ADV}}(y) = \frac{3\alpha}{4y^2}, \quad (3.8)$$

and the above equation can be written in the form analogous to that before as

$$\frac{6\alpha}{f^*(\alpha)} \frac{dW}{dy} - \frac{8i\omega_P y^2}{f^*(\alpha)} W = \frac{d}{dy} \left[ y \frac{dW}{dy} \right]. \quad (3.9)$$

Further similarity can be seen by substituting for the radial variable  $x=1/y$  then we have

$$-\frac{6\alpha}{f^*(\alpha)} \frac{dW}{dx} - \frac{8i\omega_P}{f^*(\alpha)x^4} W = \frac{d}{dx} \left[ x \frac{dW}{dx} \right]. \quad (3.10)$$

One difference that can be noted is that the tilt is advected outwards, unlike the previous isothermal disc with a radially varying density distribution (vanishing at the inner boundary), where the tilt was advected inwards. The solutions of these equations can be used as a check on how well the time-dependent code works and more importantly here, give a disc profile to make qualitative statements about  $\epsilon$  Aur.

In the earlier normalization of the disc tilt equation (see PI), we took

$$\frac{H}{H_*} = \left( \frac{R}{R_*} \right)^g \left[ 1 - \left( \frac{R_*}{R} \right)^{1/2} \right]^{1/2} \quad (3.11)$$

to avoid singularities at the inner boundary. Then the viscosity  $\nu=0$  at the inner edge. Here however it is finite, and instrumental in transporting angular momentum from the close binary. taking  $g=1$  gives

$$h = h_* \sqrt{1-1/y} \quad (3.12)$$

which for  $y \gg 1$  gives  $h \approx h_*$ . This value of  $g$  then gives the same behaviour for the tilt equation at large radii. Only near the inner boundary is a different qualitative behaviour expected.  $g=5/4$  gives  $\Sigma \propto R^{-1}$  as in the model here, but has a different opening angle behaviour.

#### 4 Numerical results and discussion

The tilt equation derived in a previous section was solved by explicit integration outwards using a finite difference scheme. This result was checked using a Runge–Kutta routine. If the precession frequency,  $\omega_P \propto x^P$  then the coefficient of  $W$  in the precession term  $\propto x^{(P-4)}$ . If we include (as before) the effects of the different precession terms by writing

$$c = \frac{6\alpha}{f^*(\alpha)}$$

and

$$c_i = -\frac{8i\sigma_0}{f^*(\alpha)},$$

then the steady state twist equation becomes

$$-C \frac{dW}{dx} + \sum_{i=1}^M c_i x^{(P_i-4)} W = \frac{d}{dx} \left[ x \frac{dW}{dx} \right]. \quad (4.1)$$

As a check on the accuracy of the results, the coordinate  $y = (R/R_*)^{1/2}$  was also used. Here the twist equation becomes

$$C \frac{dW}{dy} + \sum_{i=1}^M c_i y^{(2-P_i)} W = \frac{d}{dy} \left[ y \frac{dW}{dy} \right]. \quad (4.2)$$

Just as in the previous cases, we write this as a pair of first-order equations

$$\frac{dW}{dx} = \frac{V}{x}; \quad \frac{dV}{dx} = -\frac{CV}{x} + \sum_{i=1}^M c_i x^{(P_i-4)} W \quad (4.3)$$

and use the finite difference scheme. However, the boundary condition is different from the trivial condition earlier for the torque vanishing at this boundary. If we assume that the torque due to the twist vanishes, then  $V_{\text{in}} = -CW_{\text{in}}$  in the  $x$ -coordinates. That is, even though the binary feeds angular momentum on to a planar disc, there is none in the other directions in a twisted disc. Alternatively, the disc can be taken to be aligned at the inner boundary because the binary angular momentum is fed on to the inner boundary and it is not clear how the twisting torques here could be affected. So we have  $W_{\text{in}} = 0$ , but  $V_{\text{in}}$  has a small finite value to start the integration procedure. Because of the linearity of the equations, we can choose any  $V_{\text{in}}$  and in the end write  $W_j = W_j/W_0$ , where  $W_0$  is the computed value at the outer radius of the disc, and  $W_j$  is the value at the grid point  $x_j$ .

Three precession terms enter the equation: forced precession, recession of nodes and the quadrupole moment of the close binary. Along with the value of  $\alpha$  and the outer radius, there are five parameters. It is again not possible to explore all possibilities, but values suitable to  $\epsilon$  Aur can be used to restrict the variation. Unlike the case of a disc driven solely by Lense–Thirring precession or the close binary quadrupole moment, here the extent of the outer radius matters. The forced precession and the node recession terms scale as  $(a/a_2)^{3/2}$  and  $(a/a_2)^3$ , respectively, where  $a_2$  is the larger binary separation and  $R_0 \ll a_2$ . From the time-scale plots (Fig. 1), for  $\alpha = 10^{-2}$  and 1, respectively, we see that for the expected radius of the circumbinary disc  $\sim 2 \times 10^2$ , for  $\alpha = 1$  complete disc alignment could be expected; whereas for  $\alpha = 10^{-2}$ ,  $T_{\text{DIFF}} > T_{\text{PREC}}$  for  $R \sim R_0$ . It is not clear then whether alignment does take place and what the alignment radius is. We can expect a more complicated behaviour of the alignment radius than that based on the diffusion and precession time-scale balance. This is because the inner boundary condition ensures that the disc aligns itself even in the absence of any precession. In fact this is even more so when the condition  $W_{\text{in}} = -CV_{\text{in}}$  is used.

For small  $\alpha$ ,  $f(\alpha) \sim 1/\alpha$  is large, so that  $C, c_i \sim 0$ . The disc behaviour is then determined essentially by the equation  $[xW^1]^1 = 0$ ;  $' \equiv d/dx$  or more accurately by

$$-CW^1 = (xW^1)^1 \quad (4.4)$$

if the radial extent is large. The solution of the latter equation is

$$W = \frac{x^{-c} - 1}{x_{\text{OUT}}^c - 1} \quad (4.5)$$

using the boundary conditions  $W_{\text{in}} = 0, W_0 = 1$ . Now for small  $\alpha$ ,  $\text{Re}f(\alpha) \gg \text{Im}f(\alpha)$ , so that  $\text{Re} C \gg \text{Im} C$  and we do not expect a large phase change. It is interesting to note the behaviour of a



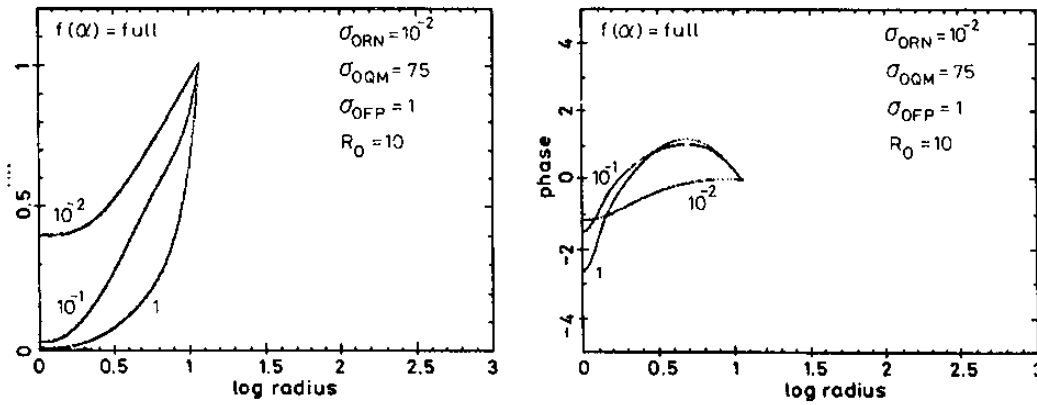


**Figure 3.** (a) and (b) The case when the inner radius is larger by a factor of 10. Note the tilt curve for  $\alpha=1/10$  which shows the effect of the outer advection of the tilt.

Different sets of values are used due to numerical reasons. We find that there is a large difference between  $\alpha=10^{-1}$  and  $\alpha=1$  for the full  $f(\alpha)$  plot, even though  $f(\alpha)$  does not vary much. This is probably due to the outer advection of the tilt. It is interesting to consider the effect of variation in  $R_0$ . In  $\epsilon$  Aur where the disc extent is uncertain, this is relevant. Fig. 3 (a) and (b) show alignment when  $R_0=10$ . The precession parameters change accordingly. We see that significant alignment takes place here as well when  $\alpha=1$ .

### 5 Appearance of the twisted disc profile

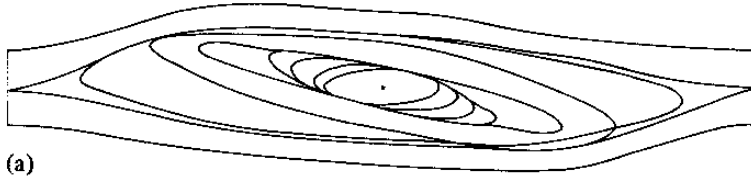
From the previous section, we have the following estimates:

$$\sigma_{ORN} \sim 10^{-5} \left( 10^2 \frac{a}{a_2} \right)^3, \quad \sigma_{OFFP} \sim \frac{1}{40} \left( 2 \times 10^2 \frac{a}{a_2} \right)^{3/2}$$

while  $\sigma_{OQM} \leq 75$ . Observational estimates are that  $R_0 \geq 2 \times 10^2$ . We see that for  $\alpha=1$ , we can have almost complete alignment of the disc with the close binary. This is observationally relevant as an aligned disc precessing along with the close binary which is inclined at  $\geq 20^\circ$  to the larger orbital plane, can produce sufficient thickness of the disc in the line-of-sight. An aspect ratio of 10:1 to 4:1 required by the observations is then provided by this disc. To this extent, it confirms the triple model for  $\epsilon$  Aur (Eggleton & Pringle 1985). This point can also be extended to SS 433 to vindicate the triple model for this object (Davidson & McCray 1980; Fabian *et al.* 1986).

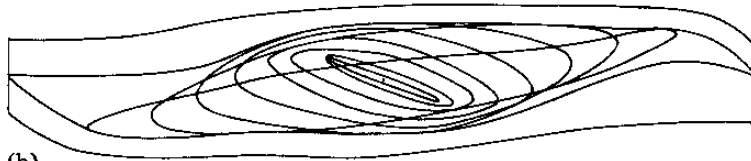
Using these parameters we trace out a twisted disc, which when seen edge-on shows a slightly contorted slab-like profile (Fig. 4). The two views, both edge-on, differ by a phase of  $90^\circ$ . The close binary inclination angle is taken to be  $20^\circ$  (i.e.  $|W|=0$  corresponds to  $20^\circ$ ). With this choice, we find an aspect ratio of approximately 5:1. By choosing a  $10^\circ$  inclination we would get an aspect ratio of approximately 10:1. This is because the twist equation is linear. Note that the disc opening angle here has been assumed to be 1/10. The outer profile, near  $R_0$  makes this clear. For a cool isothermal disc with temperature  $T \approx 500$  K, we find  $0.02 \leq H/R \leq 0.2$  for the parameters used here so that  $H/R=0.1$  is a reasonable choice. Though  $R_0=2 \times 10^2$  has been used, a much smaller value could also be used since existence of the inner binary and its separation have not been established. The choice of Kemp *et al.* (1987) corresponds to  $R_0 \approx 50$ , whereas van Hamme & Wilson (1987) used  $R_0 \approx 2-5$ . The shallow turn-on in the middle of the eclipse could be accounted for by a hole in the middle, which is conceivable in the present model. This feature could also be accounted for by a disc, which, viewed edge-on, appears with a slight constriction in the middle region rather than a bulge (Pringle 1986, private communication).

View 1: the twisted disc viewed edge-on ( $\alpha=1$ )



(a)

View 2: view1 rotated 90° clockwise ( $\alpha=1$ )



(b)

**Figure 4.** (a) and (b) The edge-on view of the disc is shown based on the results shown in Fig. 2 for  $\alpha=1$ . They show two different views 90° out of phase as would appear to an observer sitting on the outer boundary of the disc. The close binary sees a periodic variation but the primary sees only the profile in (a). The slab-like profile is similar to that used in modelling the light curve in  $\epsilon$  Aur. In both views, the outer profile takes into account of the disc opening angle, here 0.1. The inner ellipses show only the equatorial rings at each radius, with their phases fixed by the disc alignment due to precession. If a smaller value of close binary inclination were chosen, a more slender slab profile obtains. This is easily calculated due to the linearity of the twist equation. Note that here even with no tilt, a slab results with an aspect ratio of 10:1. If the opening angle were substantially reduced, say to 0.01, then the disc would be even more warped, with a much larger ratio of the central bulge to the thickness at the outer radius. The extent of the central bulge will increase as well since the alignment radius moves out due to the increase of the dimensionless frequency,  $\sigma_0 \propto (H/R)^{-1}$ .

The use of a twisted disc model is appropriate because viscous effects are directly taken into account. Since the mass loss from the companion has not taken place for a long time in the triple evolutionary scenario, the accretion disc has had time to settle into a steady state (i.e. both the surface density distribution and the disc twist are determined by their steady-state equations). It is not clear at present what the dynamics of a disc composed of a large number of particles with precessing non-circular orbits is. In particular, the viscosity effects from radial incursions or excursions of these particles are not yet clearly understood.

## 6 Conclusion

We studied the behaviour of a twisted, circumbinary disc and found that for values of the viscosity parameter  $\alpha=1$ , the disc is aligned with respect to the close binary. This disc, when viewed edge-on, is very much like the slabs and plane-inclined discs used to model the eclipse light feature of  $\epsilon$  Aur. The use of a twisted disc model is convenient because viscous effects are directly taken into account, and because a steady-state model is simpler to handle than one requiring time-dependent dynamics of a large number of particles. However, in considering large angle tilts in applications as here, the formal requirement of the theory that the tilt angle be less than the disc opening angle is not strictly adhered to.

## Acknowledgments

I thank J. E. Pringle for guidance and encouragement; P. P. Eggleton, A. C. Fabian, D. N. C. Lin, M. J. Rees and R. C. Smith for helpful discussions; the referee for constructive suggestions; D. Block and C. Godfrey for the figures.

This work was supported by a grant from the Lundgren Fund and a Research Studentship from Trinity College, Cambridge.

## References

- Backman, D. *et al.*, 1984. *Astrophys. J.*, **284**, 799.  
Davidson, K. & McCray, R., 1980. *Astrophys. J.*, **241**, 1082.  
Eggleton, P. P. & Pringle, J. E., 1985. *Astrophys. J.*, **288**, 275.  
Fabian, A. C., Eggleton, P. P., Hut, P. & Pringle, J. E., 1986. *Astrophys. J.*, **305**, 333.  
Hatchett, S. P., Begelman, M. C. & Sarazin, C. L., 1981. *Astrophys. J.*, **247**, 677.  
Huang, S.-S., 1965. *Astrophys. J.*, **141**, 976.  
Kemp, J. C. *et al.*, 1986. *Astrophys. J.*, **300**, L11.  
Kumar, S., 1985. *PhD thesis*, Univesity of Cambridge.  
Kumar, S., 1986. *Mon. Not. R. astr. Soc.*, **223**, 225.  
Kumar, S. & Pringle, J. E., 1985. *Mon. Not. R. astr. Soc.*, **213**, 435.  
Lin, D. N. C. & Papaloizou, J., 1979. *Mon. Not. R. astr. Soc.*, **188**, 191.  
Lissauer, J. & Backman, D., 1984. *Astrophys. J.*, **286**, L39.  
McLaughlin, D. B., *Astr. J.*, **67**, 117.  
Morris, S. C., 1962. *Jl R. astr. Soc. Can.*, **56**, 210.  
Papaloizou, J. C. B. & Pringle, J. E., 1983. *Mon. Not. R. astr. Soc.*, **202**, 1181.  
van Hamme, W. & Wilson, R. E., 1987. *Astrophys. J.*, submitted.  
van der Kamp, P., 1978. *Astr. J.*, **83**, 975.  
Wilson, R. E., 1971. *Astrophys. J.*, **170**, 529.

